Supporting Information (SI)

to

Electrochemistry-assisted Surface Plasmon Resonance Detection of miRNA-145 at Femtomolar Level

José A. Ribeiro[*, a], M. Goreti F. Sales[b], Carlos M. Pereira[*, a]

[a)] *CIQUP/Department of Chemistry and Biochemistry, Faculty of Sciences of University of Porto*

Rua do Campo Alegre 687, s/n, Porto 4169-007, Portugal

[b)] *BioMark/CEB-UM, Polytechnic Institute of Porto (ISEP)*

Rua Dr. António Bernardino de Almeida 431, Porto 4249-015, Portugal

*) **Corresponding Author**

E-mail: jose.ribeiro@fc.up.pt (J.A. Ribeiro), cmpereir@fc.up.pt (C.M. Pereira).

Experimental Section

Chemicals and solutions

The chemicals used throughout this work were: hydrochloric acid (37%, Sigma-Aldrich), sodium dodecyl sulfate (SDS, ≥99.0%, Merck), absolute ethanol (AGA), immersion oil (Cargille), sodium hydroxide (≥98%, Sigma-Aldrich), tris(hydroxymethyl)aminomethane (Tris, p.a., Merck), sodium chloride (≥99%, Sigma-Aldrich), magnesium chloride hexahydrate (p.a., Riedel-de Haën) and 2-mercaptoethanol (ME, purum, Fluka).

All aqueous solutions were prepared using water purified with a Milli-Q purification system (resistivity ≥18MΩ cm).

In order to minimize RNAase action and prevent miRNA degradation, the following protocol was adopted: (1) all glassware and buffer solutions were previously autoclaved (20 min, 120 °C, 1 bar) before use; (2) disposable plastic material (pipette tips, tubes, eppendorfs, etc.) was used and free from DNAases, RNAases and proteases; (3) 384 microwells SPR plates were previously immersed in solutions of 1 M NaOH and then 25% HNO_3 and finally rinsed thoroughly with pure water to prevent contamination.

Instrumentation

The hybridization studies were conducted using a SPR Autolab ESPRIT (KEI bv, The Netherlands) controlled by KEI SPR Data Acquisition software (version 4.4). The instrument consists of two independent measurement channels and incorporates a robotic auto-sampler to inject all solutions used. Solutions were aspirated from any position of the 384 microwells plate or from two available stock positions (for two different buffers). Together with the buffer flask solution, three different buffers can be added to the SPR cuvette using full-automated sequences. Solutions were injected into the measuring channels through two sharp needles that control the volume, frequency and mixing speed, for specified incubation time. In a typical experiment, 50 µL of sample solution were injected into the cuvette channels and the needles provided a continuous flow of solution over the SPR gold surface (pumping speed of 12.5 µL s^{-1}) by continuous aspiration-

dispense cycles using a mix volume of 15 µL. The cuvette is connected to a pump to drain out the liquid from the measuring channels.

Prior to the SPR experiments, the flat glass disks coated with a thin gold film (≈50 nm, KEI bv, the Netherlands) were washed thoroughly with pure water and ethanol, followed by drying under N_2 flow. The SPR gold disks were then placed over the half-cylinder glass prism covered with a thin layer of refractive-index-matching oil and stand positioned inside the equipment in a Kretschmann optical configuration [1] to begin the measurements of the SPR reflected angle (in milidegrees, m°). Gallium-Arsenide (Ga-As) diode laser acted as a source with a fixed wavelength of 670 nm in combination with a scanning mirror to modulate the angle of incidence of plane polarized light beam on the SPR substrate.

The SPR Autolab ESPRIT allows to perform electrochemical measurements in one of the two channels controlled by an external potentiostat. Simultaneous electrochemical-optical measurements (eSPR) were carried out in the electrochemical cuvette cell coupled to a conventional three-electrode configuration system. The standard SPR gold chip was used as working electrode, an unshielded Pt bar was used as counter electrode and a Ag/AgCl (saturated KCl) wire as reference electrode. Electrochemical data were obtained using a computer-controlled potentiostat Autolab PGSTAT30 (Eco Chemie B.V., Utrecht, Netherlands) monitored by the NOVA 1.11 software package.

The temperature of the SPR cell was maintained constant and reproducible by using a Julabo F32-HE (Germany) water bath. All experiments were carried out at 25.0 °C, unless otherwise stated.

As a routine procedure, all buffer solutions were degassed before use to avoid any disturbance caused by air bubbles present at the SPR sensor surface. Furthermore, the following solutions: (1) 0.5% SDS aqueous solution, (2) 100 mM HCl, (3) ethanol, (4) 100 mM NaOH and finally (5) pure H_2O were passed through the SPR flow system (≈50 mL each) prior to the beginning of the measurements to keep it free of RNAases [2, 3].

Scheme S1

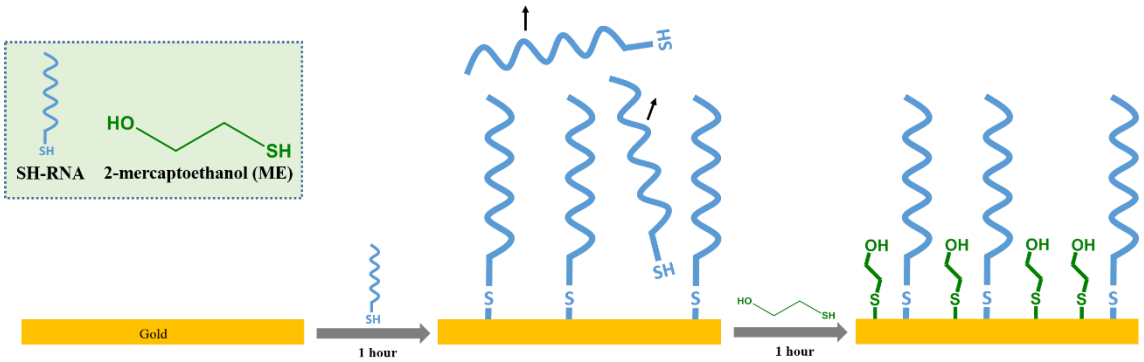

Scheme S1. Schematic representation showing the different steps involved in the modification of the SPR gold substrates, first, by immobilization of thiolated RNA strands on the sensor surface, follow immobilization of secondary thiol ME to reduce non-specific binding.

Figure S1

Maximum degree of surface coverage was estimated by performing three successive injections of 1 µM SH-RNA solution over the same gold SPR substrate.

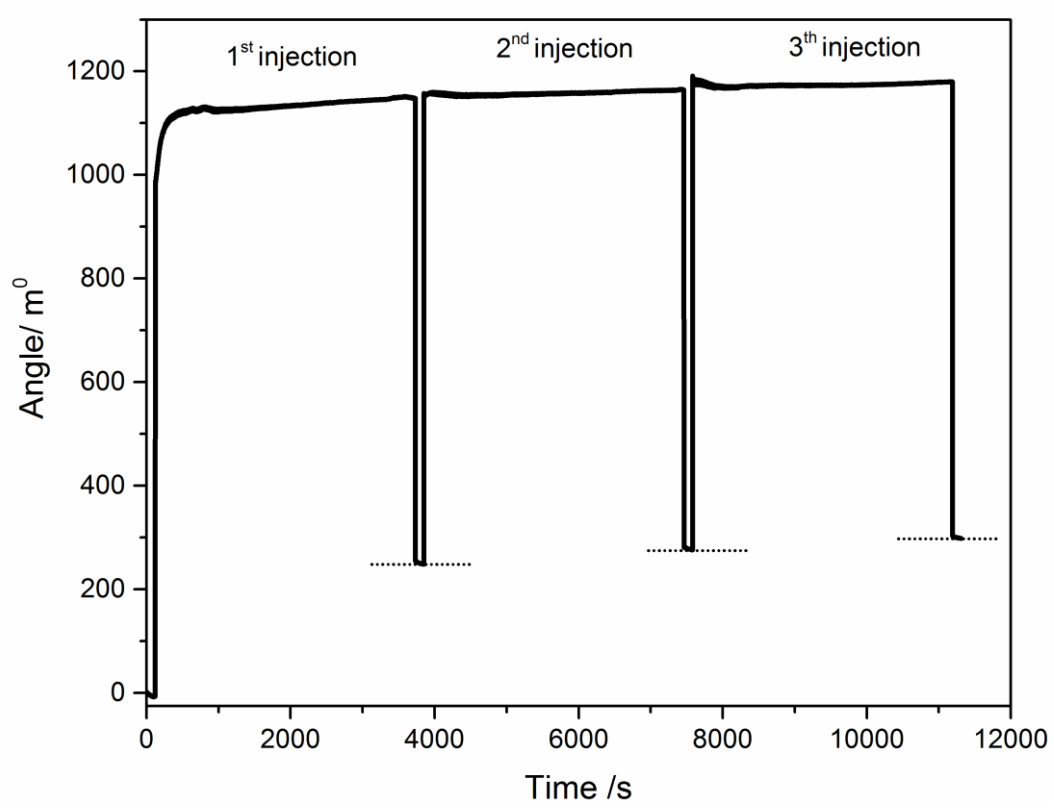

Fig. S1. Representative sensorgram obtained for maximum surface coverage estimation by multiple 1-hour injections of 1 µM SH-RNA probe solution. The arrows indicate the injections of buffer solution into the measuring system.

- Angle variation after three successive (1h) injections of SH-RNA (maximum surface coverage; n > 3): 323 ± 14 mº. *n* represents the number of experiments performed;
- Angle variation after one (1-hour) injection (n > 3): 239 ± 36 mº (corresponds to 63 % - 85 % of maximum surface coverage).

Considering that theoretical full surface coverage corresponds to ~8×10^{13} probes cm^{-2}, as reported by Steel *et al.*[4] for the assembly of ssDNA probes with thiol terminus at gold surfaces, the obtained 1-hour average surface coverage (~6×10^{13} probes cm^{-2}) used for sensor surface preparation is close to maximum. This value is in the same order of magnitude as those measured by different techniques (~4×10^{13} and ~1×10^{13} probes cm^{-2}, before and after surface treatment with MCH, respectively)[4, 5] using similar probe length, probe concentration and immobilization medium.

Figure S2

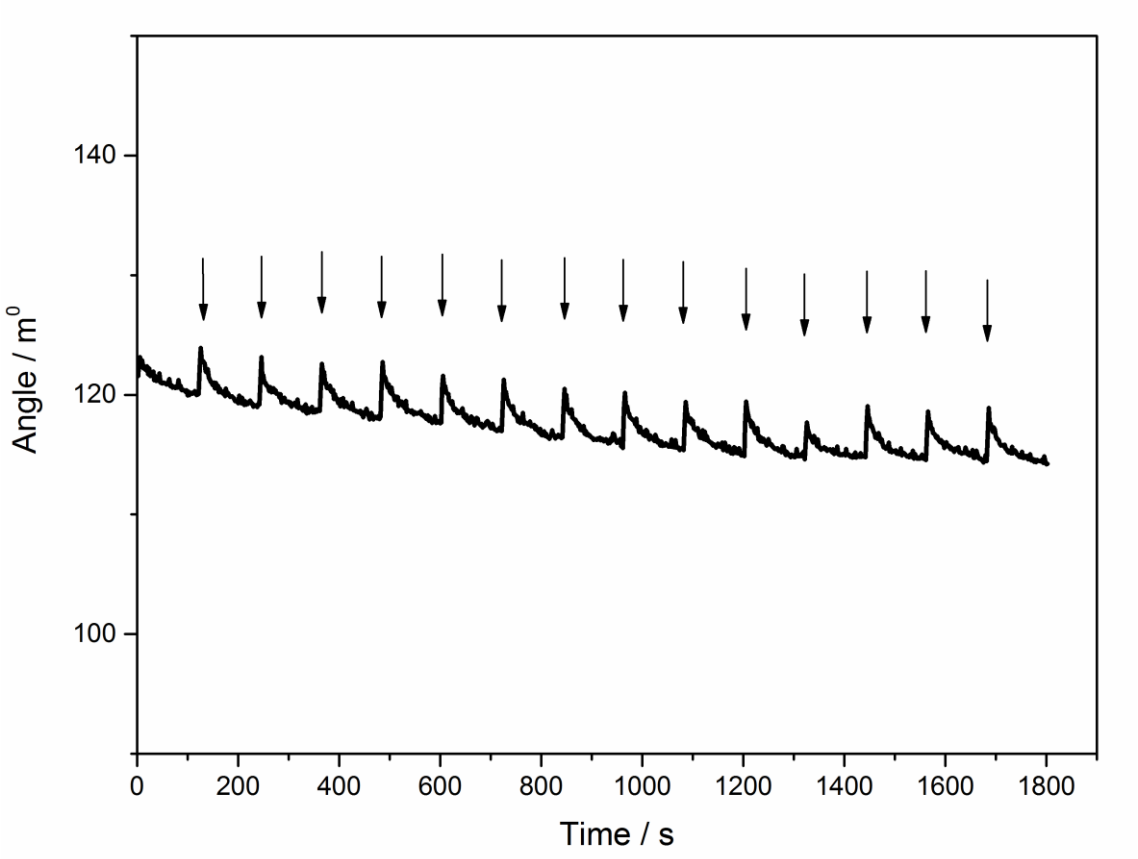

Fig. S2. Representative SPR gold surface stabilization process after surface modification with SH-RNA and ME by successive injections of 10 mM Tris-HCl buffer solution, pH 7.4, 10 mM NaCl, at 120s intervals, for 1800s. The arrows indicate the injections of buffer solution into the measuring system.

The obtained baselines are stable and reproducible over time meaning that the modification process was successful.

Figure S3

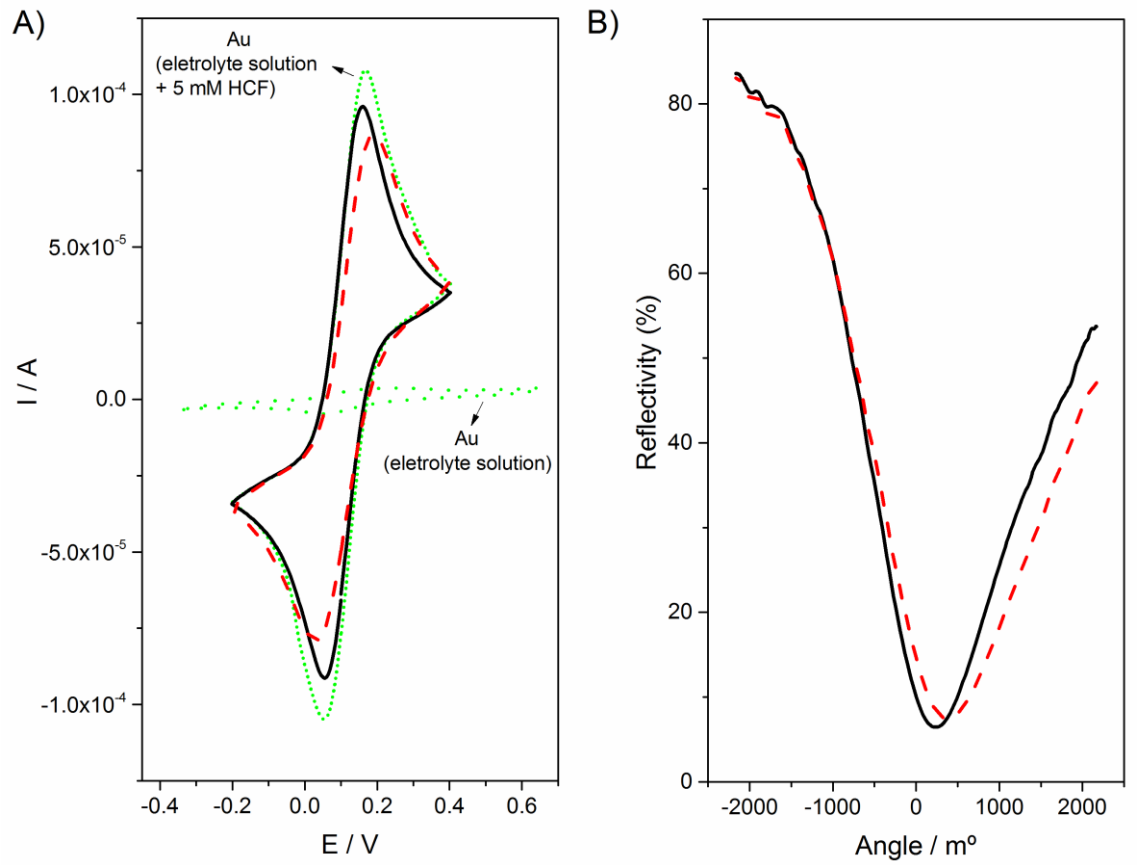

Fig. S3. (A) CVs and (B) SPR curves collected at the SPR gold surface modified with SH-RNA and ME (——) before and (---) after hybridization with 150 nM miRNA-145. For comparison, voltammograms collected at the bare SPR gold surface were also included in the figure.

Figure S4

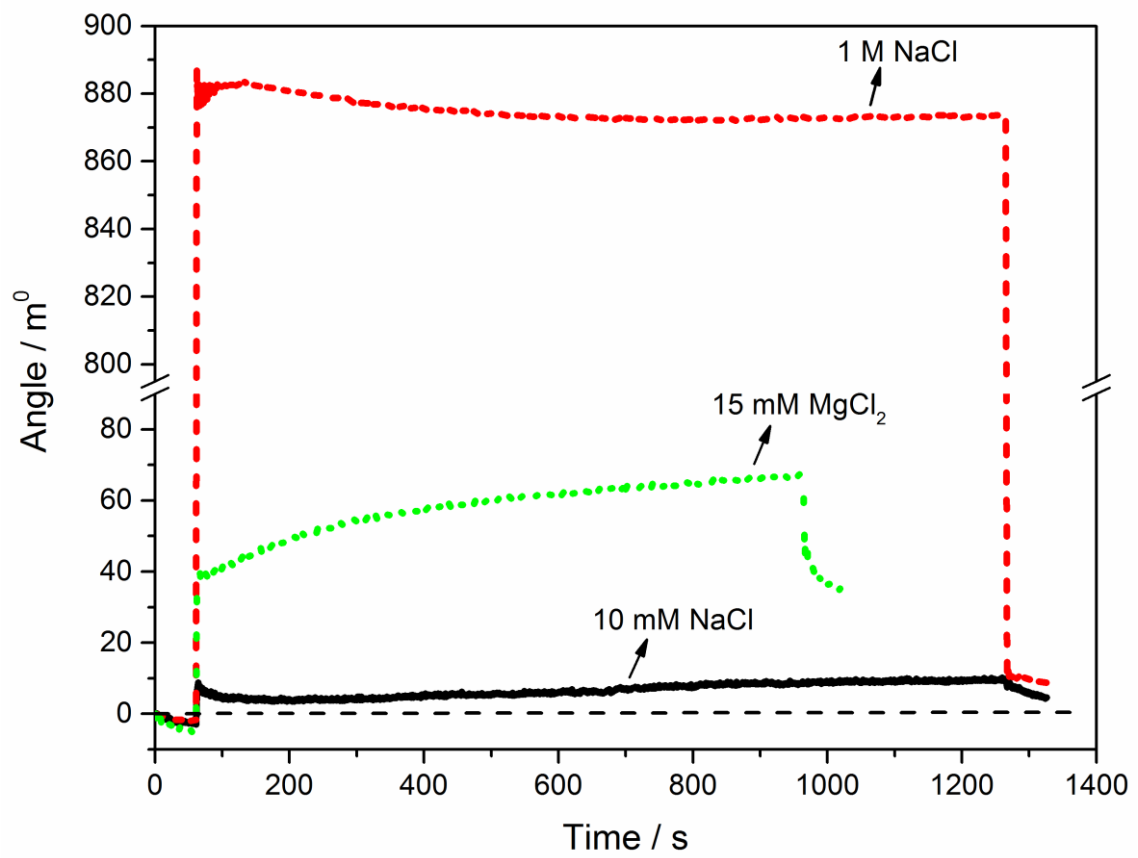

Fig. S4. Real-time SPR response to 150 mM miRNA-145 dissolved in the three hybridization buffers tested: 10 mM Tris-HCl buffer solution, pH 7.4, containing (——) 10 mM NaCl, (---) 1 M NaCl or (···) 15 mM $MgCl_2$. Line 1: baseline collected in 10 mM Tris-HCl buffer solution, pH 7.4, 10 mM NaCl, for 60s; Line 2: real-time monitoring of the interaction between surface immobilized RNA with 150 mM miRNA; Line 3: wash with Tris-HCl buffer solution for 60s (return to baseline).

The SPR angle variation obtained, after surface wash with background solution to remove unbound miRNA-145, were the following for the three buffers tested:

- Tris-HCl buffer solution, 10 mM NaCl: 7.3 m°;
- Tris-HCl buffer solution, 1 M NaCl: 10 m°;
- Tris-HCl buffer solution, 15 mM $MgCl_2$: 43 m°.

Figure S5

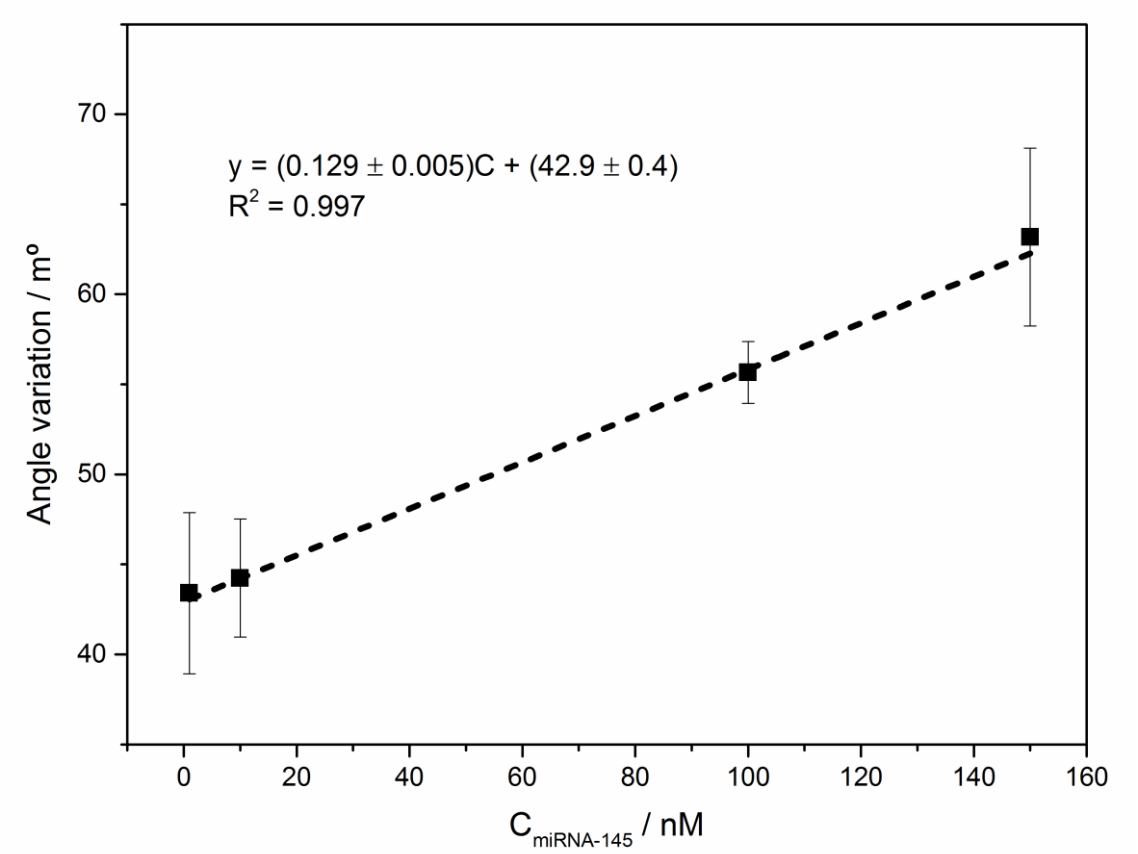

Fig. S5. Graphical representation of the angle variation as a function of the miRNA-145 concentration (from 1.0 to 150 nM).

Figure S6

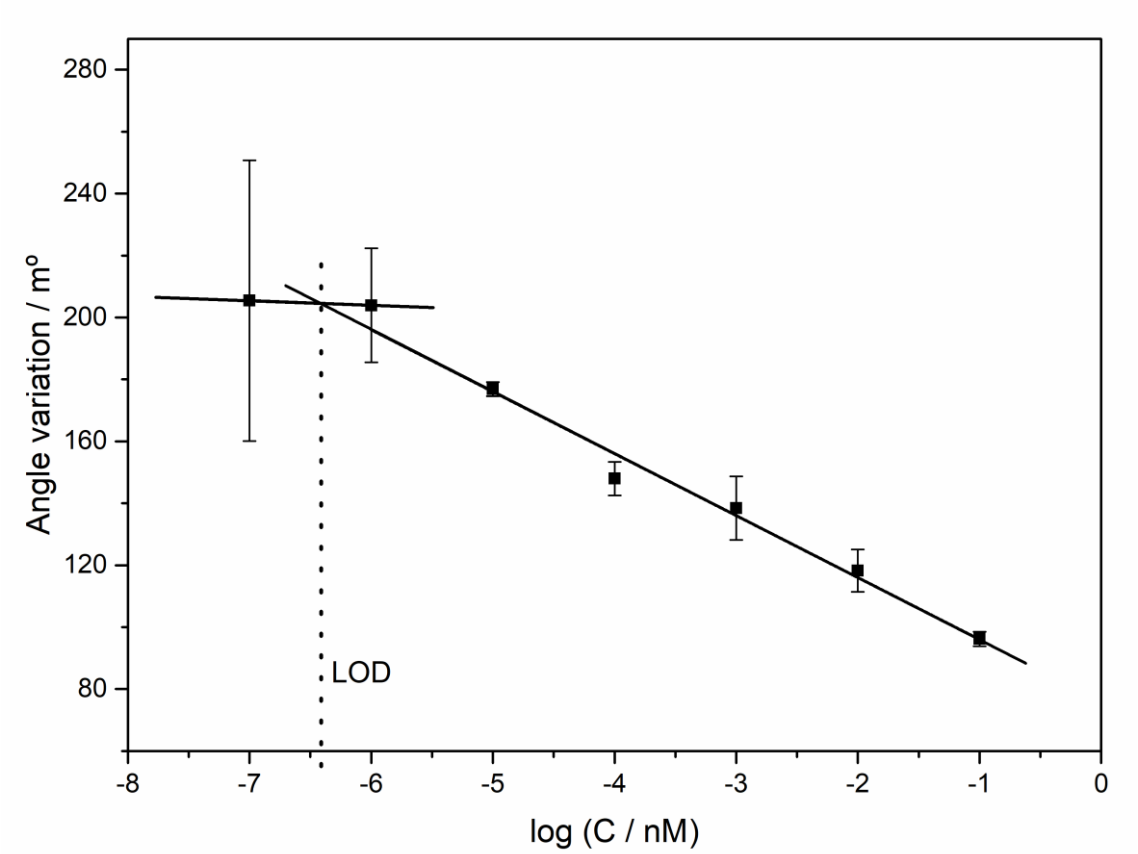

Fig. S6. LOD estimation in this work following the Recommendations of IUPAC for ion-selective electrodes.

Detection methodologies reported in literature for miRNA detection

Table S1. Analytical performance of other methodologies reported in the literature for miRNA detection

Detection method	Amplification strategy	Concentration range	LOD	Ref.
SPR	Antimonene nanosheets/AuNR-ssDNA complex	10^{-17} to 10^{-11} M	10 aM	[6]
SPR	Triple-helix formation	2 to 30 nM	1 to 3 nM	[3]
SPR	Antibody-enhanced/enzymatic	10 pM to 1 μM	1 pM/1 fM	[7]
SPR	AuNPs coupled with DNA supersandwich	0.1 to 150 pM	8 fM	[8]
eSPR	MB-labeled structure-switching DNA stem-loop	0.1 to 1500 nM	5 nM	[9]
SPR	DNA*RNA antibody	10 to 100 pM	2 pM	[10]
SPR	Multiple amplification strategy	0.1 to 10 pM	0.6 fM	[11]
SPRimaging	AuNPs amplification	0.1 to 500 pM	0.5 pM	[12]
SPRimaging	DNA-modified SiNPs	100 fM to 10 pM	100 fM	[13]
Fluorescence	Cascade signal amplification strategy	10 pM–10 nM	3.2 pM	[14]
Fluorescence	RCA	25 fM to 2.5 pM	10 fM	[15]
Colorimetry	EXPAR-assisted AuNP amplification	50 fM to 10 nM	~46 fM	[16]
ECL	ERET	100 fM to 100 nM	21.7 fM	[17]
Electrochemical	CHA and HCR	10 fM to 1 nM	3.3 fM	[18]
Electrochemical	Dual-amplification of AuNPs	100 fM to 10 pM	45 fM	[19]
Electrochemical	Electrocatalytic enzyme label	100 fM to 70 pM	60 fM	[20]
Electrochemical	RuO_2 NP-initiated deposition of an insulating film	6.0 fM to 2.0 pM	~3.0 fM	[21]
Electrochemical	DSN	2.0 fM to 2.0 pM	1.0 fM	[22]
Electrochemical	Pd NMEs (with $Ru[(NH_3)_6]^{3+}/[Fe(CN)_6]^{3-}$ system)	10 to 100 aM	10 aM	[23]
Electrochemical	Oligonucleotide encapsulated Ag-NCs	100 fM to 10 nM	67 fM	[24]
Electrochemical	---	10 aM to 1.0 nM	5.7 aM	[25]
Electrochemical	AuNPs-decorated MoS_2 nanocomposites	10 fM to 1 nM	0.78 fM	[26]
eSPR	Potential-induced deposition of a redox probe	1 fM to 10 nM	0.56 fM	This work

MB: methylene blue; RCA: rolling-circle amplification; ECL: electrochemiluminescence; EXPAR: isothermal exponential amplification reaction; ERET: electrochemiluminescence resonance energy transfer; CHA: catalyzed hairpin assembly reaction; HCR: hybridization chain reaction; DNS: duplex-specific nuclease; NMEs: nanostructured microelectrodes; Ag-NCs: silver nanoclusters;

Figure S7

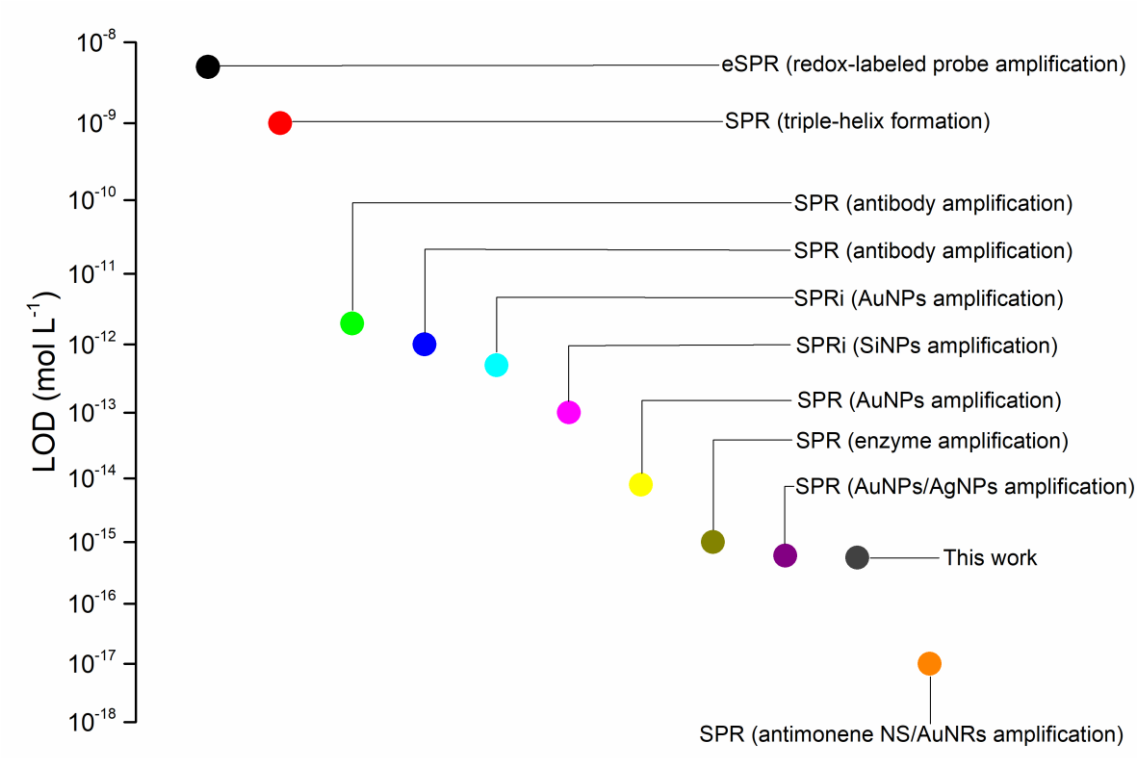

Fig. S7. Comparison of the LOD of the eSPR biosensor with other SPR methodologies reported in the literature for miRNA detection.

Figure S8

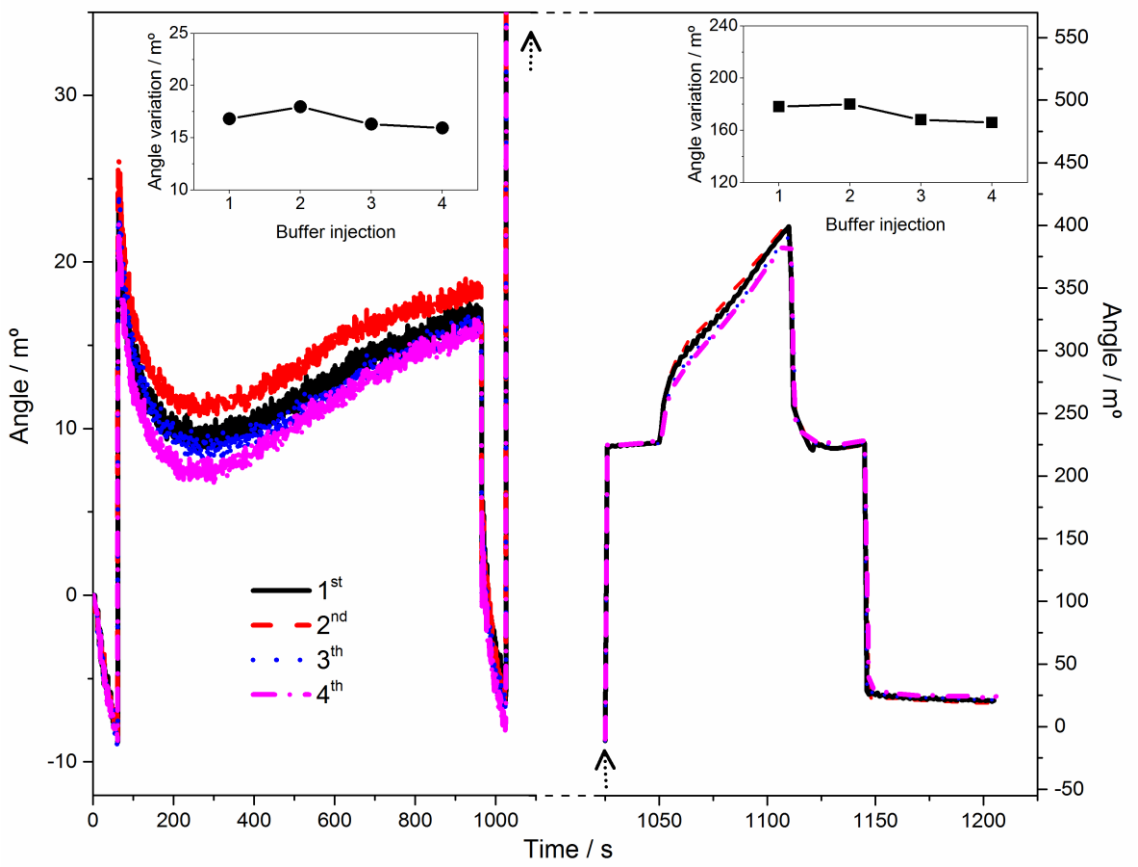

Fig. S8. Real-time SPR response (left) followed by eSPR measurements in the presence of 5 mM ferro/ferricyanide redox probe solution (right) collected at the sensor surface with immobilized RNA strands, after four successive injections of hybridization buffer solution (10 mM Tris-HCl buffer solution, pH 7.4, 15 mM $MgCl_2$, without miRNA-145) to the measuring channel. Insets: SPR equilibrium angle variation (left) and potential-induced SPR angle variation (right) obtained after each buffer solution injection.

- SPR equilibrium angle variation (n = 4): 16.8 ± 0.8 m°
- eSPR angle variation (n = 4): 173 ± 6 m°

Figure S9

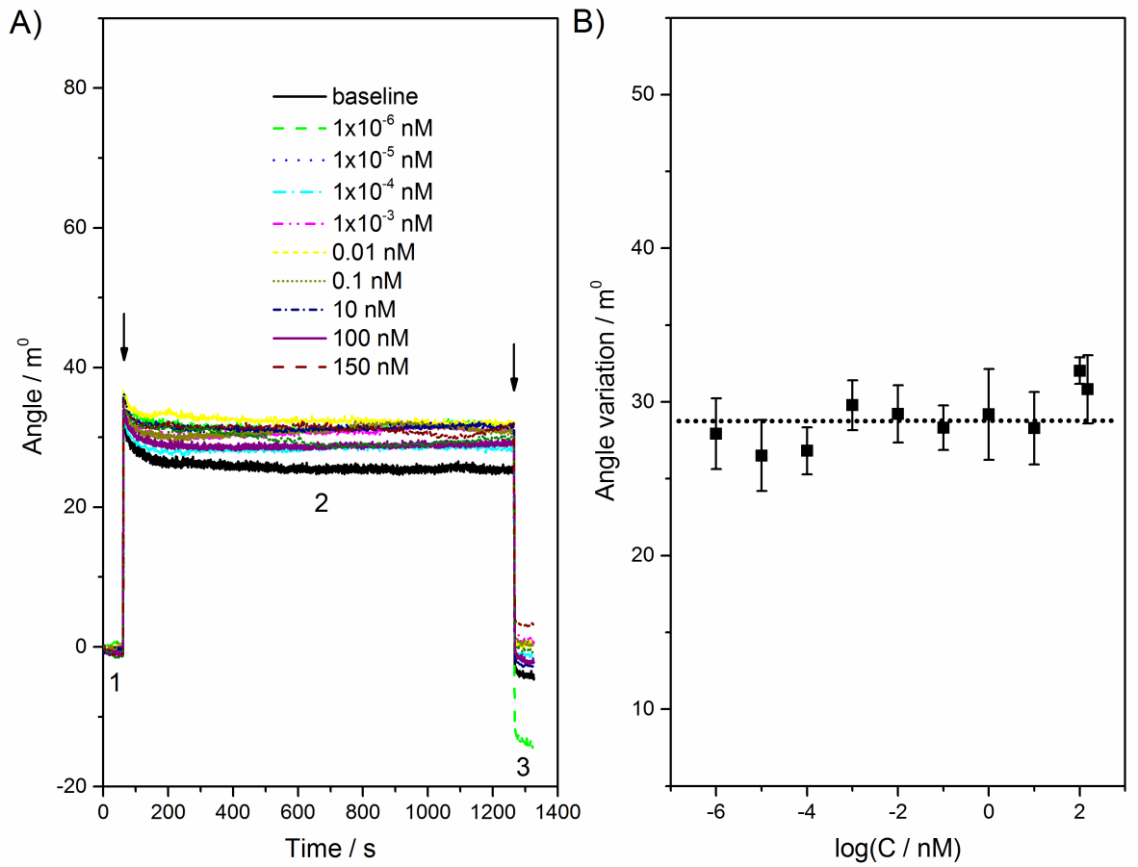

Fig. S9. (A) Real-time SPR monitoring of the interaction between immobilized RNA strands on gold substrates and non-complementary (NC) miRNA fragments. The concentrations of NC miRNA tested ranged from 1.0 fM to 150 nM. Line 1: baseline collected in 10 mM Tris-HCl buffer solution, pH 7.4, 10 mM NaCl, for 60s; Line 2: real-time monitoring of the interaction between surface immobilized RNA with NC miRNA for 20min; Line 3: wash with Tris-HCl buffer solution for 60s (return to baseline). For comparison, the response obtained after injection of hybridization buffer (without NC miRNA) into the measuring channel (dashed line) is also shown in the figure. The arrows indicate the injection of the different solutions into the measuring system. (B) Graphical representation of the angle variation as a function of the logarithm of NC miRNA concentration obtained under conditions of SPR hybridization equilibrium.

- Non-complementary (NC) miRNA sequence: 5´-CCG AUC GCA GGG UCC AUU AAA GA-3´

eSPR measurements performed during hybridization phase

eSPR measurements were performed during the hybridization phase of the SPR biosensing experiment in order to improve the detection sensitivity of the binding event, without the need of a redox probe. In this context, two approaches were tested, the application of an electric potential to eSPR cuvette and perform CV cycles, during the hybridization phase.

Application of an electric potential

Electrostatic charging can enhance hybridization events, as reported elsewhere [27]. In this work, an electrostatic field (E = +0.3 V) was applied to the eSPR cell and held for several minutes to investigate the effect of electrostatic charging on the interactions between surface-bound thiolated RNA and target miRNA fragments in solution. The current resulting from the electrostatic field is limited to capacitive non-Faradaic charging current.

Initial experiments were performed with hybridization buffer (electrolyte solution), without containing miRNA-145, as shown in Fig. S10. As can be seen, the SPR angle instantly increases after application of the electrostatic field due to the fast adsorption of negatively charged species at the sensor surface modified with the RNA monolayer. After that, the SPR angle slowly increases over the potential/time regime applied. When the potential is turned off, desorption occurs and the SPR angle decreases. However, a much higher decrease of the SPR signal was expected, revealing poor reversibility of potential-induced changes occurred at the sensor surface. Furthermore, after washing the surface with background solution, the baseline shifted to higher values, indicating that surface initial conditions where not restored. Thus, CV measurements were tested aiming to overcome the above-mentioned limitations.

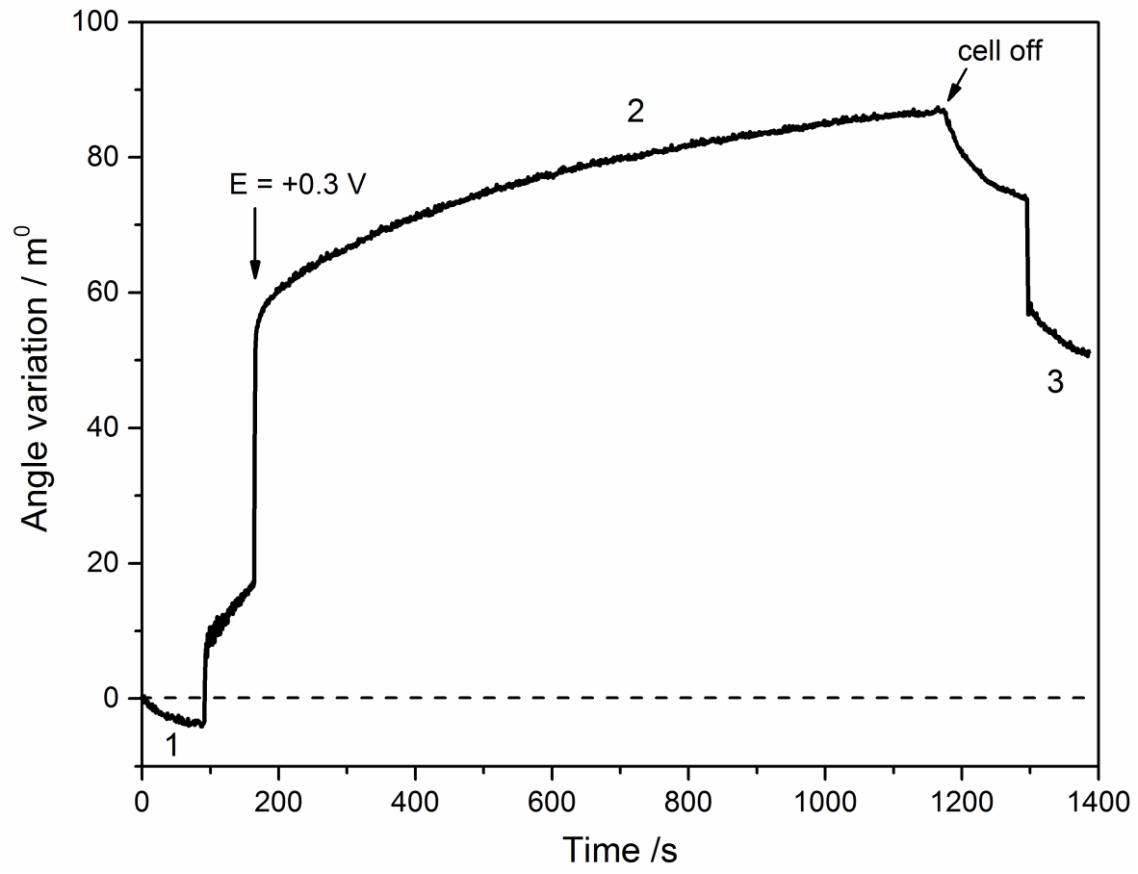

Fig. S10. Application of an electric potential during the hybridization phase of the SPR experiment. Line 1: baseline collected in 10 mM Tris-HCl buffer solution, pH 7.4, 10 mM NaCl, for 90s; Line 2: injection of hybridization buffer (without miRNA-145) into the measuring channel for 20min. After 75s equilibration at open circuit, the potential of +0.3 V (*vs.* Ag/AgCl) was applied to the eSPR cell and held for 1000s, after which the applied field is turned off. Line 3: wash with Tris-HCl buffer solution for 90s (return to baseline).

Aplication of Cyclic Voltametry technique

CV measurements were performed aiming to control the adsorption/desorption processes occurring at the sensor surface. The potential limits of CV, between -0.3 and 0.3 V, are within the ideally polarizable region of the gold electrode. They were carefully selected to promote repetitive adsorption/desorption cycles of species at the sensor surface, instead of massive adsorption when an electrostatic field is applied. In principle, positive potentials applied in the forward scan (see inset of Fig. S11) should promote hybridization of (negatively charged) target miRNA in solution with complementary surface-immobilized strands. By opposition, the negative potentials applied in backward scan induces desorption of non-specific bound molecules from the sensor surface, without denaturation of duplexes formed.

The CV-assisted SPR investigations performed with hybridization buffer used, without containing miRNA-145, are shown in Fig. S11. The CVs collected with the SPR gold substrates containing the immobilized thiolated RNA (inset of Fig. S11) show that only capacitive charging currents were obtained.

Although the CVs performed allowed establishing several sequential adsorption/desorption equilibrium processes between electrolyte solution ions and the gold substrate, the SPR angle measured tends to increase until it reaches saturation, revealing that adsorption in not fully reversible. In addition, after washing the sensor surface with background solution the surface initial conditions were not fully restore. Further studies are needed to understand adsorption phenomena occurring at the RNA modified-sensor surfaces under electrochemical control.

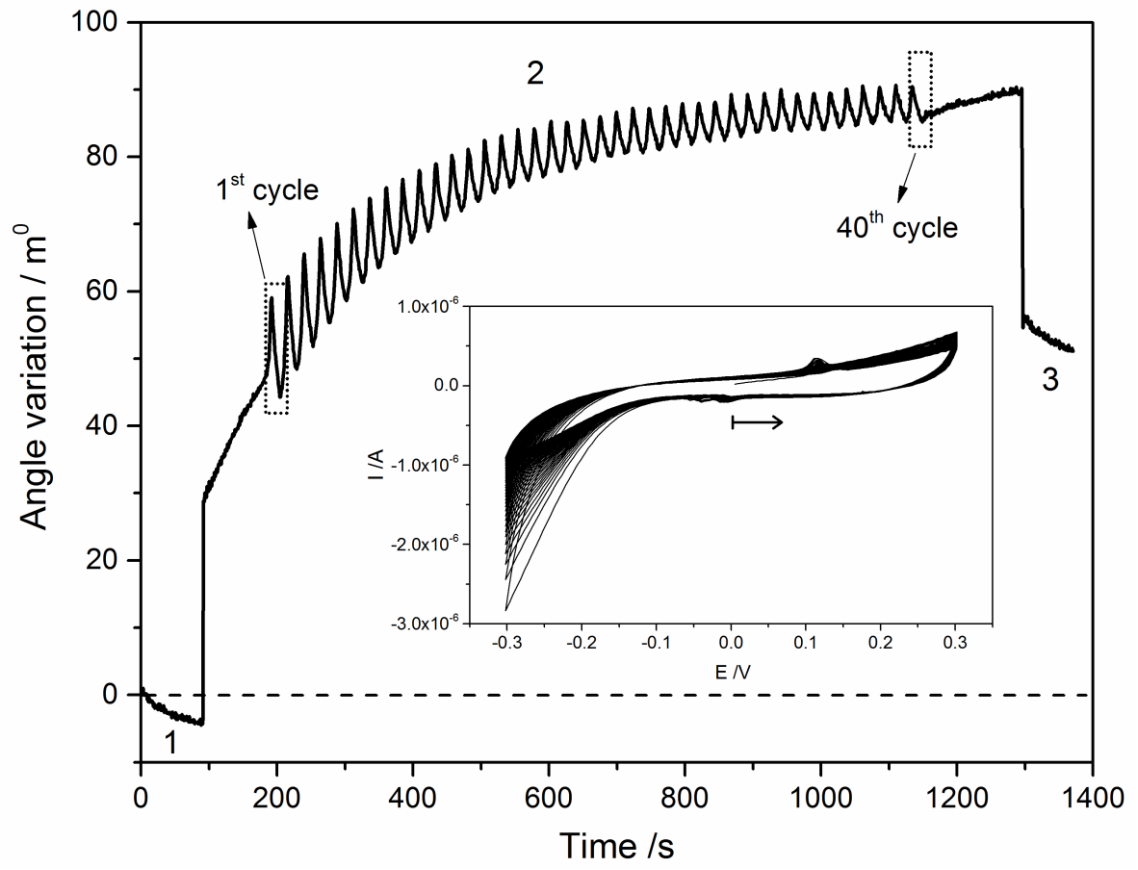

Fig. S11. CV measurements performed during the hybridization phase of the SPR experiment. Line 1: baseline collected in 10 mM Tris-HCl buffer solution, pH 7.4, 10 mM NaCl, for 90s; Line 2: injection of hybridization buffer (without miRNA-145) into the measuring channel for 20min. After 75s equilibration, the 40 CV cycles were collected between -0.3 and 0.3 V. Line 3: wash with Tris-HCl buffer solution 90s (return to baseline). Inset: Voltammograms recorded in 10 mM Tris-HCl buffer solution, pH 7.4, 15 mM $MgCl_2$, at 50 mV s^{-1}, with the modified SPR gold substrate.

References

[1] A. Kausaite, M. van Dijk, J. Castrop, A. Ramanaviciene, J.P. Baltrus, J. Acaite, A. Ramanavicius, Surface plasmon resonance label-free monitoring of antibody antigen interactions in real time, Biochemistry and Molecular Biology Education 35(1) (2007) 57-63.

[2] L.G. Carrascosa, S. Gómez-Montes, A. Aviñó, A. Nadal, M. Pla, R. Eritja, L.M. Lechuga, Sensitive and label-free biosensing of RNA with predicted secondary structures by a triplex affinity capture method, Nucleic Acids Research 40(8) (2012) e56-e56.

[3] A. Aviñó, C.S. Huertas, L.M. Lechuga, R. Eritja, Sensitive and label-free detection of miRNA-145 by triplex formation, Analytical and Bioanalytical Chemistry 408(3) (2016) 885-893.

[4] A.B. Steel, R.L. Levicky, T.M. Herne, M.J. Tarlov, Immobilization of nucleic acids at solid surfaces: Effect of oligonucleotide length on layer assembly, Biophysical Journal 79(2) (2000) 975-981.

[5] A.W. Peterson, R.J. Heaton, R.M. Georgiadis, The effect of surface probe density on DNA hybridization, Nucleic Acids Research 29(24) (2001) 5163-5168.

[6] T. Xue, W. Liang, Y. Li, Y. Sun, Y. Xiang, Y. Zhang, Z. Dai, Y. Duo, L. Wu, K. Qi, B.N. Shivananju, L. Zhang, X. Cui, H. Zhang, Q. Bao, Ultrasensitive detection of miRNA with an antimonene-based surface plasmon resonance sensor, Nature Communications 10(1) (2019) 28.

[7] S. Schmieder, J. Weisspflog, N. Danz, M. Hubner, S. Kreth, U. Klotzbach, F. Sonntag, Ultrasensitive SPR detection of miRNA-93 using antibody-enhanced and enzymatic signal amplification, Engineering in Life Sciences 17(12) (2017) 1264-1270.

[8] Q. Wang, R.J. Liu, X.H. Yang, K.M. Wang, J.Q. Zhu, L.L. He, Q. Li, Surface plasmon resonance biosensor for enzyme-free amplified microRNA detection based on gold nanoparticles and DNA supersandwich, Sensors and Actuators B-Chemical 223 (2016) 613-620.

[9] A.M. Dallaire, S. Patskovsky, A. Vallee-Belisle, M. Meunier, Electrochemical plasmonic sensing system for highly selective multiplexed detection of biomolecules based on redox nanoswitches, Biosensors & Bioelectronics 71 (2015) 75-81.

[10] H. Sipova, S.L. Zhang, A.M. Dudley, D. Galas, K. Wang, J. Homola, Surface Plasmon Resonance Biosensor for Rapid Label-Free Detection of Microribonucleic Acid at Subfemtomole Level, Analytical Chemistry 82(24) (2010) 10110-10115.

[11] R.J. Liu, Q. Wang, Q. Li, X.H. Yang, K.M. Wang, W.Y. Nie, Surface plasmon resonance biosensor for sensitive detection of microRNA and cancer cell using multiple signal amplification strategy, Biosensors & Bioelectronics 87 (2017) 433-438.
[12] H. Vaisocherova, H. Sipova, I. Visova, M. Bockova, T. Springer, M.L. Ermini, X. Song, Z. Krejcik, L. Chrastinova, O. Pastva, K. Pimkova, M.D. Merkerova, J.E. Dyr, J. Homola, Rapid and sensitive detection of multiple microRNAs in cell lysate by low-fouling surface plasmon resonance biosensor, Biosensors & Bioelectronics 70 (2015) 226-231.
[13] W.J. Zhou, Y.L. Chen, R.M. Corn, Ultrasensitive Microarray Detection of Short RNA Sequences with Enzymatically Modified Nanoparticles and Surface Plasmon Resonance Imaging Measurements, Analytical Chemistry 83(10) (2011) 3897-3902.
[14] R. Wang, L. Wang, H.Y. Zhao, W. Jiang, A split recognition mode combined with cascade signal amplification strategy for highly specific, sensitive detection of microRNA, Biosensors & Bioelectronics 86 (2016) 834-839.
[15] Y.Q. Cheng, X. Zhang, Z.P. Li, X.X. Jiao, Y.C. Wang, Y.L. Zhang, Highly Sensitive Determination of microRNA Using Target-Primed and Branched Rolling-Circle Amplification, Angewandte Chemie-International Edition 48(18) (2009) 3268-3272.
[16] R.D. Li, B.C. Yin, B.C. Ye, Ultrasensitive, colorimetric detection of microRNAs based on isothermal exponential amplification reaction-assisted gold nanoparticle amplification, Biosensors & Bioelectronics 86 (2016) 1011-1016.
[17] Y. Cheng, J.P. Lei, Y.L. Chen, H.X. Ju, Highly selective detection of microRNA based on distance-dependent electrochemiluminescence resonance energy transfer between CdTe nanocrystals and Au nanoclusters, Biosensors & Bioelectronics 51 (2014) 431-436.
[18] X.Y. Wu, Y.Q. Chai, R. Yuan, Y. Zhuo, Y. Chen, Dual signal amplification strategy for enzyme-free electrochemical detection of microRNAs, Sensors and Actuators B-Chemical 203 (2014) 296-302.
[19] N. Xia, L.P. Zhang, G.F. Wang, Q.Q. Feng, L. Liu, Label-free and sensitive strategy for microRNAs detection based on the formation of boronate ester bonds and the dual-amplification of gold nanoparticles, Biosensors & Bioelectronics 47 (2013) 461-466.
[20] H.S. Yin, Y.L. Zhou, H.X. Zhang, X.M. Meng, S.Y. Ai, Electrochemical determination of microRNA-21 based on graphene, LNA integrated molecular beacon, AuNPs and biotin multifunctional bio bar codes and enzymatic assay system, Biosensors & Bioelectronics 33(1) (2012) 247-253.

[21] Y.F. Peng, Z.Q. Gao, Amplified Detection of MicroRNA Based on Ruthenium Oxide Nanoparticle-Initiated Deposition of an Insulating Film, Analytical Chemistry 83(3) (2011) 820-827.
[22] Y.Q. Ren, H.M. Deng, W. Shen, Z.Q. Gao, A Highly Sensitive and Selective Electrochemical Biosensor for Direct Detection of MicroRNAs in Serum, Analytical Chemistry 85(9) (2013) 4784-4789.
[23] H. Yang, A. Hui, G. Pampalakis, L. Soleymani, F.F. Liu, E.H. Sargent, S.O. Kelley, Direct, Electronic MicroRNA Detection for the Rapid Determination of Differential Expression Profiles, Angewandte Chemie-International Edition 48(45) (2009) 8461-8464.
[24] H.F. Dong, S. Jin, H.X. Ju, K.H. Hao, L.P. Xu, H.T. Lu, X.J. Zhang, Trace and Label-Free MicroRNA Detection Using Oligonucleotide Encapsulated Silver Nanoclusters as Probes, Analytical Chemistry 84(20) (2012) 8670-8674.
[25] A.R. Cardoso, F.T.C. Moreira, R. Fernandes, M.G.F. Sales, Novel and simple electrochemical biosensor monitoring attomolar levels of miRNA-155 in breast cancer, Biosensors & Bioelectronics 80 (2016) 621-630.
[26] S. Su, W.F. Cao, W. Liu, Z.W. Lu, D. Zhu, J. Chao, L.X. Weng, L.H. Wang, C.H. Fan, Dual-mode electrochemical analysis of microRNA-21 using gold nanoparticle-decorated MoS2 nanosheet, Biosensors & Bioelectronics 94 (2017) 552-559.
[27] R.J. Heaton, A.W. Peterson, R.M. Georgiadis, Electrostatic surface plasmon resonance: Direct electric field-induced hybridization and denaturation in monolayer nucleic acid films and label-free discrimination of base mismatches, Proceedings of the National Academy of Sciences of the United States of America 98(7) (2001) 3701-3704.